

# RISE – E2E SIMULATOR FOR THE GENERATION OF USER DEFINED SPECTRAL IMAGING DATA SETS

Johannes Schmidt<sup>1\*</sup>, Johanna dall'Amico<sup>1</sup>, Bernhard Sang<sup>1</sup>, Roger Förstner<sup>2</sup>

<sup>1</sup>OHB System AG, Image Simulation & Processing, 82234 Weßling, Germany

<sup>2</sup>Universität der Bundeswehr, Institute of Space Technology and Space Applications, 85577 Neubiberg, Germany

## ABSTRACT

Current end-to-end (E2E) simulators support the development of satellite missions in various ways including the evaluation of technical requirements and the assessment of preliminary instrument performance. However, most E2E simulators are designed to be instrument-specific and are incapable of depicting the entire processing chain. This paper introduces a *generic* simulator, the Remote Sensing Image Simulation Environment (RISE), capable of covering a large spectrum of remote sensing applications. The generic design of RISE offers the user full control of every processing step including the simulation of real ground-truth to ground-truth data and instrument behaviour. Consequently, users can generate training data, necessary for deep learning (DL) algorithms in remote sensing applications, with substantially improved quality. RISE comprises a geometry module (GM), scene generation module (SGM), sensor module (SM), as well as Level 1 (L1) and Level 2 (L2) processing modules, which are currently under development.

**Index Terms**— remote sensing, multi – and hyperspectral, E2E, deep learning, training data

## 1. INTRODUCTION

Hyper – and multispectral instruments are primarily used on airborne and satellite missions for numerous Earth observation tasks. The mechanism of imaging spectroscopy is one of the fastest-growing research areas in remote sensing as it enables the separation of physical, chemical and biological components of the observed target. The analysis of each component provides quantitative products and services applicable to the fields of agriculture, food security, raw materials, soils, biodiversity, environmental and atmospheric observation, as well as forestry. The expanding demand from science institutions and commercial sectors for applications in agricultural, resource and environmental management, drives the development and planning of hyper-/multispectral spaceborne systems ready to be launched within the next few years. [1]

Simulators fundamentally contribute to the design of new spaceborne systems as they allow technical and

performance requirements to be assessed [2]. These simulators can be divided into several modules:

- *Geometry Module*, modelling the observation geometry
- *Retrievals Module*, modelling the bio-geophysical parameters
- *Scene Generation Module*, distributing the bio-geophysical parameters over an artificial scene
- *Sensor Module*, modelling the sensor behaviour
- *Level 1 Processor*, applying radiometric, spectral and spatial corrections
- *Level 2 Processor*, applying the atmospheric correction algorithms and conversion to bio-geophysical parameters
- *Level 3 Processor*, using the bio-geophysical parameters for further applications.

Simulators vary significantly in their coverage of those modules. The standalone modules MODTRAN [3] and 6S [4] are deployed for atmospheric simulations included in the SGM. Retrieval modules such as OSIRIS [5], Prospect [6], WASI [7] and the four-stream-model [8] [9] are already well established and tested. In the field of E2E simulators, the EnMAP simulator, EETES [10], SENSOR [11], PRISMA simulator [12] and others have been developed to comprise all aforementioned modules. However, these E2E simulators are non-generic (i.e. designed to be instrument/mission-specific) and/or incapable of simulating from ground-truth to ground-truth level.

Another field with rising importance is image and signal processing. The increasing complexity and dimensionality of hyper – and multispectral data, mixed pixels, light scattering mechanisms as well as atmospheric and geometric distortions make the produced data inherently non-linear. Effective processing of those data sets has become a major challenge. Therefore, several research fields including *classification, spectral unmixing, dimensionality reduction, resolution enhancement, denoising and restoration* have gained considerable attention. At present, many processing methods make use of DL algorithms [13] [14].

The generic RISE simulator fills two research gaps in the field of image processing:

- (1) RISE will provide a “real” generic E2E simulator, capable of simulating a variety of different missions/instruments and,
- (2) RISE will have the capability of producing “real” ground-truth to ground-truth data with the user having control of all simulation parameters, which enhances training algorithms for DL methods.

This paper gives a brief overview of the planned RISE simulator and the chosen generic approach. The next section presents a summary of the design and architecture of the modules comprising RISE in addition to their current implementation and validation status. The application of the RISE S/W in the field of DL training algorithms is, based on denoising algorithms, described in section 4. Section 5 describes preliminary outputs retrieved by the S/W. Finally, a summary and outlook are given in the last section.

## 2. RISE – OVERVIEW

E2E simulators are capable of simulating ground-truth to ground-truth data up to L2. In order to keep the simulators as generic and modular as possible E2E simulators are divided into separate main modules in line with ESA’s ARCHEO-E2E study [2]: *Geometry Module, Scene Generator, Instrument/Sensor Module, Level 1 Processing and Level 2 Retrieval*. This setup allows RISE to simulate passive optical remote sensing applications.

### 2.1. Main Modules

The RISE simulator adapts principles of the general design, according to the ARCHEO study [2], which allows the software to cover a wide range of remote sensing applications (see Figure 1).

- *Geometry Module:*  
In charge of calculating the S/Cs real and estimated orbit and attitude as well as the observation geometry (line of sight). It supports various orbit definitions and mission scenarios.
- *Scene Generation Module:*  
In charge of modelling the “to-be” retrieved parameters as well as the radiative transfer forward model. The usage of a coupled soil-leaf canopy and atmosphere radiative transfer modelling will enable the application for most of the existing mission goals in terms of retrievals.
- *Sensor Module:*  
In charge of modelling the sensor in the spatial and spectral domain as well as radiometric behaviour. It accounts for sensor electronics and calculates the radiance in digital numbers (DN). At the end of the processing chain on-board-processing steps such as encryption, binning and compression can be applied. Common scanning modes such as pushbroom, step and

stare, whiskbroom are implemented and initiated by the user.

- *Level 1 Module:*  
In charge of converting DNs into physical measurements. L0 accounts for reverting possible on-board modifications/ compressions/ encryptions. L1B calculates and applies spectral and radiometric corrections based on calibration tables provided externally by the user. L1C calculates and applies geometric corrections (e.g. co-registration, orthorectification)
- *Level 2 Module:*  
In charge of calculating retrievals from top of atmosphere (TOA) reflectance. L2A accounts for atmospheric corrections through an atmospheric backward model, resulting in bottom of atmosphere (BOA) radiances. L2B converts the provided reflectance spectra in surface variables.

### 2.2. Generic Approach

The key aim of RISE is to provide an E2E framework that is “as generic as possible” and therefore, support a comprehensive range of mission/instrument specifications. Nevertheless, certain modules and sub-modules cannot be developed in a general design and must be adapted on a case-by-case basis. The GM does not require any further adaptations, while the SGM is only partially generic. For instance, the simulation of user-defined gas plumes beneath the atmosphere requires a gas plume generator to be attached to the SGM (see retrievals module in Figure 1). The SM is implemented as a generic module, which does not require any further adaptations for relevant instrument types. The L2 processor, like the SGM, is only partially generic. While L2A is implemented as a generic module, special retrieval requirements make the L2B case-specific.

## 3. RISE – DESIGN & ARCHITECTURE

The RISE simulator makes use of the proposed ARCHEO architecture, albeit with some adaptations. Figure 2 shows the generic flow diagram designed for RISE. As for all E2E simulators, the first executed module is the GM, which provides output to subsequent modules. The second step in the simulation chain is the SGM, followed by the SM. The post-processing from L0 to L2 is done as the last step in the overall processing chain. The RISE S/W is implemented in the Python environment to make use of pre-defined libraries.

### 3.1. Geometry Module

The GM is based on the previously validated BIBLOS-1 geometry module [15]. It has been slightly modified to match the required file formats of RISE. The BIBLOS-1 geometry module is composed of four blocks which are also used in

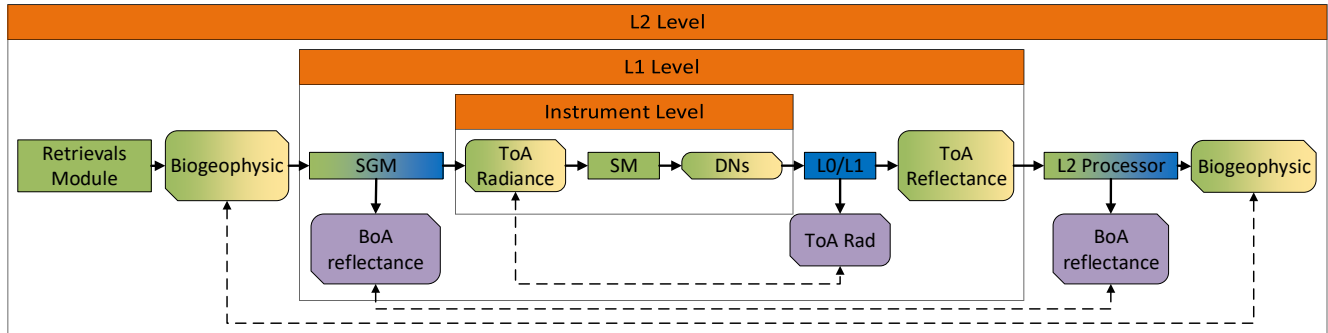


Figure 1: RISE overview

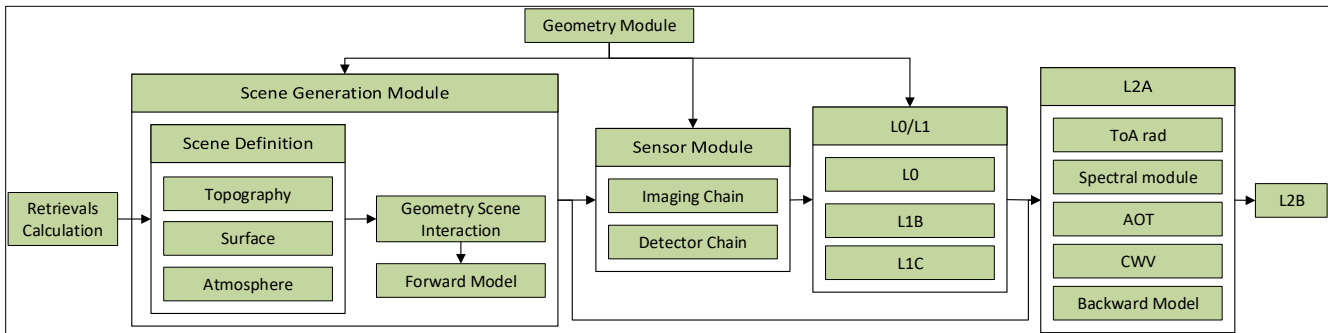


Figure 2: RISE flow diagram

RISE: *Orbit, Attitude, AOCS/Instrument coupling, Scene Interaction* [16]. The output of the GM consists of real and estimated geometry data.

### 3.2. Scene Generation Module

The generic SGM of RISE is divided into three main modules as shown in Figure 3: *Scene Definition, Geometry-Scene-Interaction, Forward Model*. The final output of the SGM, the top of atmosphere radiances, are then used by the SM.

The *scene definition* submodule is the first step of the SGM. This sub-module will distribute the key topographic, bio-geophysical and atmospheric input variables over the scene grid. It consists of *topography definition, surface definition* and *atmosphere definition*. The *topography definition* is in charge of creating the elevation map for the scene to be simulated. The elevation map is needed for the correct calculation of the illumination and viewing conditions as well as the calculation of column water vapour (CWV) and aerosol load. The *surface definition* distributes the desired surface types over each scene grid point based on provided maps. The distribution of the surface types can be performed randomly, based on user-defined classes or external databases. The *atmosphere definition* assigns the atmospheric conditions to each scene grid point. The atmosphere is characterized by a set of key atmospheric variables, such as aerosol type, aerosol optical thickness (AOT) and CWV [17]. Atmospheric profiles define the temperature, pressure and gas distribution according to the altitude profile. The aerosol definition includes the definition of aerosol type (phase

function, spectral dependence, etc.) and concentration. The CWV affects light propagation through multiple absorption bands, making it a key atmospheric parameter that is altitude-dependent. The last step of the atmosphere definition is the definition of a cloud map.

The second module, the *Geometry-Scene-Interaction*, calculates the viewing and illumination conditions for each scene grid point as well as shadow and viewing masks. The illumination conditions are defined by the solar zenith and azimuth angles. Following the algorithm described by Reda [18], the angles are calculated based on the scene's geolocation (geodetic latitude and longitude) and elevation map. The viewing conditions consist of the observation zenith and azimuth angles. They are retrieved by intersecting the provided LOS with the WGS84 Reference Ellipsoid. In order to account for an elevated surface, an iterative approach is implemented according to the BIBLOS-1 geometry module [19].

The *Forward Model* is the last module of the SGM and computes the surface reflectance and TOA radiances over each scene grid point. The calculations are based on coupled surface and atmospheric radiative transfer models (RTM) following the four-stream approach by Verhoef and Bach [8] [20]. Throughout the entire SGM, the user controls spatial and spectral resolutions in addition to simulated sub-sampling ratios.

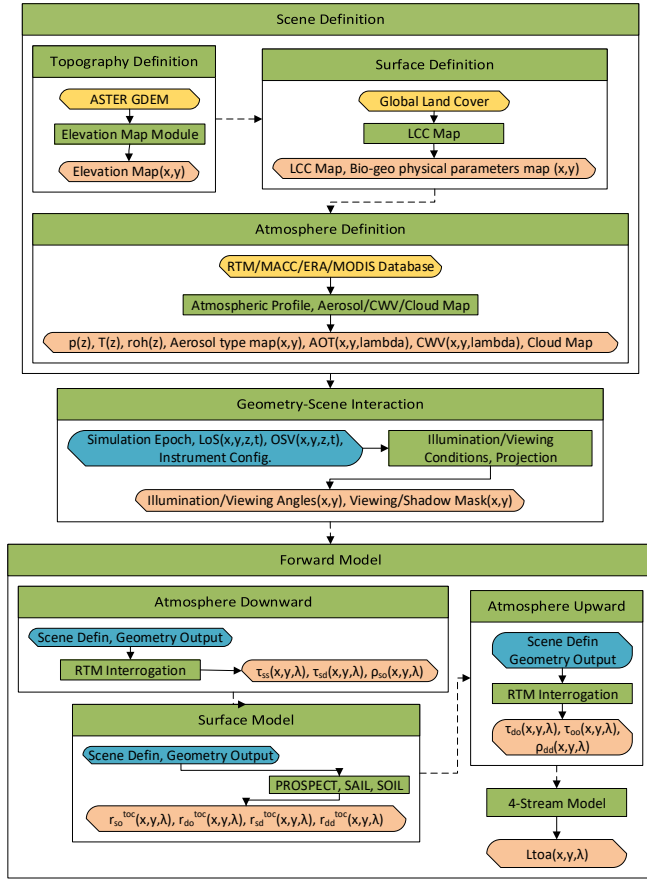


Figure 3: SGM flow diagram

### 3.3. Sensor Module

The SM of RISE will be capable of covering the following instruments and scanning modes. Three instrument types comprising multi – and hyperspectral, VHR and FFT instruments including digital and physical time-delayed integration (TDI) will be implemented. Additionally, all standard scanning modes will be covered incl. whiskbroom, pushbroom, step and stare, snapshot.

The generic SM of RISE consists of five main modules: *grid definitions*, *optical transfer function (OTF) calculations*, *imaging chain*, *detector chain* and *on-board-processing*. The *grid definition* creates, based on the selected instrument and scanning mode, all required grids for further calculations. In the case of a hyperspectral instrument, it creates the additional required frequency and spatial sampling grids as well as the imaging grid, accounting for dispersion and smile effects. The *OTF* module calculates the following instrument-specific optical transfer functions: *SpectrometerOptics*, *Detector*, *Jitter*, *Instrument*, *Imaging*, *WFE*, *Smear*. The *imaging* module propagates the incoming radiation through its optical systems. It, therefore, accounts for smile and keystone effects, slit masking and performs the convolution with the previously calculated OTFs. The last module is the

*detector* block transforming incoming irradiance on the detector to DN's in several steps. In the case of a hyperspectral instrument, the number of electrons collected by the detector is retrieved from the spectral flux. Additionally, background and dark current electrons are calculated. PRNU, DSNU, noise, DNL, INL are applied to the incoming signal and finally converted to DN's with a transfer function. The calculated DN's are then processed by the *on-board-processing module*, capable of encryption, binning and compression

Throughout the entire chain of the SM, the user controls additional errors, for example, noise contributions, which can be added as Gaussian or Poisson distributions. Moreover, the spatial and spectral resolutions as well as the simulated sub-sampling ratios are user-defined parameters.

### 3.4. L1 Processing Module

The *L1* processing module is composed of the *L1A/B* and *L1C* module and in charge of the post-processing of the acquired signal. The *L1A/B* module applies the geometric, spectral and radiometric processing, i.e. georeferencing, DN to TOA radiance conversion and resampling of spectral frames. The *L1C* module applies the orthorectification and co-registration processing. The generated TOA reflectance values are projected and resampled on a uniform grid in the WGS84/UTM reference coordinate system.

### 3.5. L2 Processing Module

The *L2* processing module is composed of the *L2A* and *L2B* module and in charge of converting the TOA input to BOA radiances applying the atmospheric correction. From the BOA radiance, the retrievals are calculated.

### 3.6. Current Status

At present, the RISE S/W is under development. Therefore, not all of the aforementioned modules and functionalities have been implemented and validated. The *GM* is fully implemented and validated. The *SGM* is about to be completed, while MODTRAN is currently being incorporated into the simulator framework. The *SM* is partially finished and validated. This means that the hyperspectral branch of the module has been developed, implemented and validated in the scope of the ESA CHIME Project Phase A/B1. Implemented but not yet validated is the multispectral branch, while the tailoring for the VHR part is currently on-going. Similarly, the *L1* modules are finished and validated apart from some minor adaptations for the VHR branch. The *L2* modules have been defined but implementation has not started.

## 4. RISE – TRAINING DATA GENERATOR

The imaging process, which is covered by the RISE framework, introduces unwanted degradation of spectral data

caused by atmospheric haze and instrumental noise. Instrumental noise, incl. thermal, quantization and shot noise, can lead to the corruption of spectral bands. Corrupted bands have a negative effect on the quality/efficiency of image-processing techniques and are therefore often removed. However, the removal of corrupted bands can potentially lead to the loss of substantial information [21].

Conventional denoising methods evolved from 2D approaches and convex optimizations to a 3D model-based method. These methods are reliable on the estimation of the noise variance and several other parameters such as dominant noise type and level *a priori* [22]. DL provides a solution to the above-mentioned issues. Zhang et al. [13] avoid complex, *a priori* constraints for image denoising by using convolutional neural networks (CNN) and were able to achieve comparable results to conventional methods. Such DL methods require intense and reliable training sets. The newly developed CNNs for denoising tasks use an image obtained by, for example, the Hyperspectral Digital Imagery Collection Experiment airborne sensor. This image (incl. residual noise) is set as the ground-truth. Additive white gaussian noise with different spectra are then imposed for training purposes. [14]

E2E simulators, covering the whole imaging process such as RISE, provide additional possibilities for training a CNN. Firstly, the SGM can provide several noise-free, artificial scenes serving as a real ground-truth reference for the CNN learning algorithm. Inside the SM, each noise contribution (signal-dependent, sparse and pattern) can be controlled and modelled individually (magnitude, Gaussian, Poisson). The output of the SM can serve as the noisy input for the learning algorithm. This approach can improve learning algorithms in terms of accuracy, and enable users to distinguish different noise types. The separately developed retrieval module (L2B) will evaluate the impact of the denoising algorithm not only on classification but on the biogeophysical parameter themselves.

## 5. RISE – RESULTS

As the E2E chain of RISE is currently under development and some modules remain incomplete, conclusive results are limited at this stage. In the scope of the ESA CHIME A/B1, the SM and L1 processing module have already been implemented and validated. Figure 4 shows an extract of the performed validation process and its results. The left image shows a uniform scene input radiance after the instruments slit. The simulated point spread function (PSF) is then applied via a convolution (`run_imaging`) resulting in the output signal in the right image. The left image in Figure 5 is an externally provided validation scene (in the scope of ESA CHIME A/B1 from GFZ [23]) that served as an input to the SM. After the SM processing chain, the output is handed to the L1B processor which performs the mosaicking (see right Figure 5).

Figure 6 shows the user-defined scene before the forward model is executed. It must be noted that the land cover class (LCC) map is created on a random distribution basis and does not represent a realistic LCC distribution.

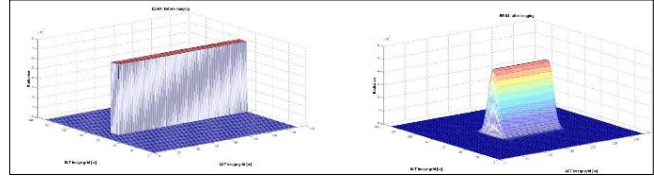


Figure 4: SM imaging chain and PSF simulation

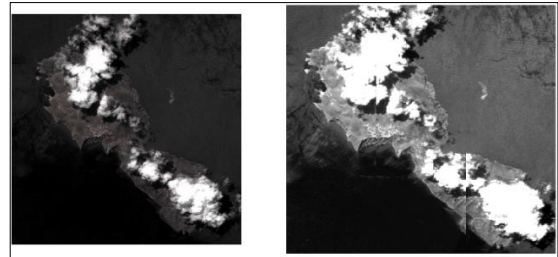


Figure 5: L1B mosaicking validation (left input, right output)

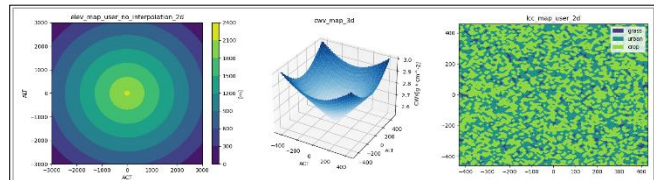


Figure 6: SGM scene preparation (from left: elevation, CWV, LCC)

## 6. CONCLUSION

The RISE simulator is designed with the capacity to support numerous instrument and mission designs as well as DL algorithms. As presented in this paper, the generic E2E design ensures the applicability and expendability of the S/W to various remote sensing applications. Currently, the SGM (the forward model) is under development, pending subsequent validation. The first version of the SGM will be capable of ingesting user-defined topography, land cover, CWV, and AOT maps. In the next version, automatic pulls of DEMs and LCC maps according to the geo-position will be implemented. The SM, covering hyperspectral instruments operating in pushbroom mode has been implemented and validated. Multispectral instruments incl. TDI, filter and splitter systems are already covered by the second version of SM but not validated yet. Currently under development is the VHR branch of the SM. Subsequently, the validation of the multispectral and VHR branches will be performed. The L1 processing modules have been implemented and validated for the hyperspectral branch. For the multispectral and VHR branch, minor adaptations are required. The L2 processing module has been analysed and preliminary ATBDs have been defined.

## 7. REFERENCES

- [1] M. Rast und T. H. Painter, *Earth Observation Imaging Spectroscopy for Terrestrial Systems: An Overview of Its History, Techniques, and Applications of Its Missions*, Bd. 40, Springer Netherlands, 2019, pp. 303-331.
- [2] C. de Negueruela, M. Scagliola und D. Guidici, „ARCHEO-E2E: A Reference Architecture for Earth Observation end-to-end Mission Performance Simulators,“ 2012.
- [3] S. M. Adler-Golden, M. W. Matthew, L. S. Bernstein, R. Y. Levine, A. Berk, S. C. Richtsmeier, P. K. Acharya, G. P. Anderson, J. W. Felde, J. A. Gardner, M. L. Hoke, L. S. Jeong, B. Pukall, A. J. Ratkowski und H.-h. K. Burke, „Atmospheric correction for shortwave spectral imagery based on MODTRAN4,“ in *Imaging Spectrometry V*, 1999.
- [4] E. F. Vermote, D. Tanré, J. Luc Deuzé, M. Herman und J.-J. Morcrette, „Second Simulation of the Satellite Signal in the Solar Spectrum, 6S: An Overview,“ 1997.
- [5] T. Pogliano, S. Mathieu-Marni, T. Ranchin, E. Savaria und L. Wald, „OSIRIS: a physically based simulation tool to improve training in thermal infrared remote sensing over urban areas at high spatial resolution,“ *OSIRIS. Remote Sensing of Environment*, Bd. 104, pp. 238-246, 2006.
- [6] S. Jacquemoud, W. Verhoef, F. Baret, C. Bacour, P. J. Zarco-Tejada, G. P. Asner, C. François und S. L. Ustin, „PROSPECT + SAIL models: A review of use for vegetation characterization,“ *Remote Sensing of Environment*, Bd. 113, Nr. SUPPL. 1, pp. 1-11, 2009.
- [7] P. Gege, „The water color simulator WASI: An integrating software tool for analysis and simulation of optical in situ spectra,“ *Computers and Geosciences*, Bd. 30, Nr. 5, pp. 523-532, 6 2004.
- [8] W. Verhoef und H. Bach, „Simulation of hyperspectral and directional radiance images using coupled biophysical and atmospheric radiative transfer models,“ *Remote Sensing of Environment*, Bd. 87, Nr. 1, pp. 23-41, 2003.
- [9] W. Verhoef und H. Bach, „Simulation of Sentinel-3 images by four-stream surface-atmosphere radiative transfer modeling in the optical and thermal domains,“ *Remote Sensing of Environment*, Bd. 120, pp. 197-207, 2012.
- [10] K. Segl, T. Küster, C. Rogaß, H. Kaufmann, B. Sang, V. Mogulsky und S. Hofer, „EeteS: An end-to-end image simulation tool applied to the EnMAP hyperspectral mission,“ in *International Geoscience and Remote Sensing Symposium (IGARSS)*, 2012.
- [11] A. Börner, L. Wiest, R. Reulke, R. Richter, P. Keller, M. Schaepman und D. Schläpfer, „SENSOR: a tool for the simulation of hyperspectral remote sensing systems,“ 2001.
- [12] A. Barducci, D. Guzzi, C. Lastris, P. Marcoionni, V. Nardino und I. Pippi, „SIMULATING THE PERFORMANCE OF THE HYPERSPECTRAL PAYLOAD OF THE PRISMA MISSION,“ 2012.
- [13] K. Zhang, W. Zuo, Y. Chen, D. Meng und L. Zhang, „Beyond a Gaussian Denoiser: Residual Learning of Deep CNN for Image Denoising,“ 13 8 2016.
- [14] A. Maffei, J. M. Haut, S. Member, M. E. Paoletti, J. Plaza, S. Member, L. Bruzone und A. Plaza, „WHISPERS: WORKSHOP ON HYPERSPECTRAL IMAGE AND SIGNAL PROCESSING: EVOLUTION IN REMOTE SENSING 1 Efficient convolutional neural network for spectral-spatial hyperspectral denoising,“ 2019.
- [15] GMV, „BIBLOS Homepage,“ GMV, [Online]. Available: <https://gmv-biblos.gmv.com/>. [Zugriff am 03 03 2021].
- [16] GMV, „GMV-BIBLOS-DD Design Definition File 1.0,“ GMV, Poland, 2016.
- [17] C. Tenjo, J. P. Rivera-Caicedo, N. Sabater, J. Vicent Servera, L. Alonso, J. Verrelst und J. Moreno, „Design of a Generic 3-D Scene Generator for Passive Optical Missions and Its Implementation for the ESA's FLEX/Sentinel-3 Tandem Mission,“ *IEEE Transactions on Geoscience and Remote Sensing*, Bd. 56, Nr. 3, pp. 1290-1307, 1 3 2018.
- [18] I. Reda und A. Andreas, „Solar Position Algorithm for Solar Radiation Applications (Revised),“ 2000.
- [19] GMV, „BIBLOS2-GMV-D4 Software Design Document 4.3,“ GMV, Poland, 2020.
- [20] W. Verhoef und H. Bach, „Coupled soil-leaf-canopy and atmosphere radiative transfer modeling to simulate hyperspectral multi-angular surface reflectance and TOA radiance data,“ *Remote Sensing of Environment*, Bd. 109, Nr. 2, pp. 166-182, 30 7 2007.
- [21] P. Ghamisi, N. Yokoya, J. Li, W. Liao, S. Liu, J. Plaza, B. Rasti und A. Plaza, *Advances in Hyperspectral Image and Signal Processing: A Comprehensive Overview of the State of the Art*, Bd. 5, Institute of Electrical and Electronics Engineers Inc., 2017, pp. 37-78.
- [22] B. Rasti, J. R. Sveinsson, M. O. Ulfarsson und J. A. Benediktsson, „HYPER-SPECTRAL IMAGE DENOISING USING 3D WAVELETS,“ 2016.
- [23] GFZ Helmholtz-Zentrum, „CHIME Validation Scenes,“ GFZ Helmholtz-Zentrum, Potsdam, 2019.